Colossal magnetoresistance using the small polaron picture with finite bandwidth effects

Sudhakar Yarlagadda
Saha Institute of Nuclear Physics, Calcutta, India
and Texas Center for Superconductivity, University of Houston, Houston, Texas 77204-5932
(Received 31 May 2000)

We present a small polaron picture and show that finite bandwidth effects are important to understand colossal magnetoresistance. Besides the polaron size parameter, we show that there is another parameter (adiabaticity parameter) that is relevant to studying magnetoresistance. We find that for fixed values of the polaron size parameter an increase in the adiabaticity parameter increases the magnetoresistance. The magnetic transition is studied within a mean-field approach. We point out important oversights in the literature. We find that for the reported values of the bandwidth (based on band-structure calculations) and for experimentally determined values of activation energy and Debye frequency, the calculated values of the magnetoresistance compare favorably with experimental ones. We calculate the optical conductivity too and find that there is reasonable agreement with experiment.

I. INTRODUCTION

Studying perovskite manganites of the form $A_{1-\delta}B_{\delta}MnO_3$ (A=La, Pr, Nd, etc.; B=Sr, Ca, Ba, etc.) as a function of doping δ has lead to a variety of rich phenomena.[1–3] Of these $La_{1-\delta}Ca_{\delta}MnO_3$ is perhaps the simplest one because the ionic size difference between La^{3+} and Ca^{2+} is less than 3%. In $La_{1-\delta}Ca_{\delta}MnO_3$, at low doping, as temperature is lowered the system undergoes orbital ordering and at even lower temperatures a layered antiferromagnetism is observed.[4] At intermediate doping ($\delta \sim 0.2-0.4$), simultaneous metal-insulator (MI) and paramagnetic-ferromagnetic transitions occur in this compound as the temperature is decreased. At even higher doping (i.e., greater than $\delta \sim 0.5$) charge ordering is realized while at $\delta \sim 1$ antiferromagnetic order results at low temperatures.[1] To explain the magnetic ordering at low doping, de Gennes[5] some time ago had proposed double-exchange mechanism wherein, on account of strong Hund's coupling between the spin of a mobile hole and the spin of the localized electrons, the hopping integral of the itinerant hole is reduced by half of the cosine of the angle between the 3/2 spins of the localized electrons on neighboring sites. Furukawa pioneered in demonstrating the usefulness of the dynamical mean-field theory in understanding the properties of double-exchange systems.[6] However it was recognized by Millis *et al.*[7] that double-exchange mechanism itself is not sufficient to explain colossal magnetoresistance (CMR). Millis and co-workers have proposed a model[8] which uses Jahn-Teller coupling between electrons and nuclei. However, this model treats phonons classically and does not seem to yield satisfactory results away from half-filling. Furthermore, these authors have studied the phenomenon using only the polaron size parameter (the ratio between the hopping integral and the binding energy). They have not studied the effect of another dimensionless parameter—the ratio between the hopping integral and the Debye frequency (adiabaticity parameter). Röder *et al.* have also stressed the importance of Jahn-Teller coupling in understanding these manganites.[9] Lee and Min have also studied polaron transport in manganites.[10] However, these authors do not take into account the renormalization of the electron-phonon interaction due to finite bandwidth effects. Jaime *et al.*[11] and Worledge *et al.*[12] have demonstrated that their high-temperature resistivity data fits well to an adiabatic small polaron model. All in all, there is growing evidence for a small polaron picture to explain CMR.

In this paper we study CMR phenomena in perovskite manganites by considering the carriers as small polarons whose high-temperature behavior is hopping type and low-temperature behavior is metal like.[13] Our model includes effects due to electron-phonon coupling and on-site Hund's coupling between itinerant holes and localized electrons. To understand the MI transition we simplify the Hamiltonian by accounting for the Hund's coupling through the double-exchange hopping term.[5] By including finite bandwidth effects, and using a suggestion by Toyozawa[14] we obtain an expression for the small polaronic wave function. Using this *nearly* small polaronic wave function we obtain the dynamic conductivity. We find that in the presence of a magnetic field both double exchange and finite bandwidth effects lower the resistivity and shift its peak to higher temperatures and thus can lead to CMR. In our picture the main reason for the CMR is due to the renormalization of the electron-phonon interaction (or the lattice distortion) due to finite bandwidth effects. One of our important conclusions is that for a fixed value of the polaron size parameter the magnetoresistance increases as the adiabaticity parameter increases.

Within a mean-field approach, we calculate the magnetization (M) of the localized spins. The magnetization M is a result of the effective magnetic field generated by the band-like motion of the electrons or in other words, the itinerant electrons due to the strong Hund's coupling polarize the localized spins. We have studied the magnetization for both with and without external magnetic fields and found that our M values are qualitatively in agreement with experimental results.[15] Furthermore our magnetoresistance values also compare favorably with experimental ones.[15]

We also calculate the optical conductivity above the metal-insulator transition temperature. We find that the optical conductivity scaled by the dc conductivity depends only on the renormalized electron-phonon coupling and the Debye frequency. We calculate optical conductivity as a function of frequency at various temperatures and find reasonable agreement with experiments.[16]

II. BACKGROUND

Earlier on Zener proposed a double-exchange model where conduction from a Mn^{3+} to a Mn^{4+} via an O^{2-} can be understood in terms of simultaneous transfer of two electrons—one electron from a Mn^{3+} to a neighboring O^{2-} and another electron from the O^{2-} to a neighboring Mn^{4+}. De Gennes further realized that since the Hund's coupling is much larger than the hopping integral t, the hopping term gets modified to be $t\cos(\theta/2)$ where θ is the angle between neighboring spins that are treated classically. More recently it was pointed out that there is a Berry phase factor that enters the hopping term.[17] However, we feel that the geometric phase will not significantly alter the basic physics behind CMR. Then to understand propagation of holes, of doping level δ, along a chain of spins (all with spin S) coupled antiferromagnetically through the coupling parameter J one needs to minimize the energy $E=-2t\delta\cos(\theta/2)+|J|S^2\cos(\theta)$ to obtain the ground state canting angle $\cos(\theta/2)=t\delta/(2|J|S^2)$.

Within a mean-field approach one can approximate $\cos(\theta)$ to be given by $\langle\vec{S}_i/S\rangle\cdot\langle\vec{S}_j/S\rangle=M^2/M_S^2$ where M/M_S is the scaled magnetization. Thus the hopping term gets modified to be $t\sqrt{(1+M^2/M_S^2)/2}$. However, this double-exchange modification of the hopping integral itself does not explain the observed metal-insulator transition in the intermediate doping regime.

To understand the colossal magnetoresistance phenomenon we will now use small polaronic picture. First we will provide the motivation for this approach. One of the striking features of a single small polaron is that the shape of the inverse of the mobility as a function of temperature is quite similar to that of the resistivity observed for the manganite systems that display colossal magnetoresistance. To understand how this comes about we will present our understanding of a small polaron first by ignoring spin effects. In systems like the transition-metal oxides the electron couples to the vibrational modes of the host molecule (say the breathing mode). Due to strong electron-phonon coupling the molecular equilibrium configuration gets distorted. The electron gets bound in the distortion to form a polaron. This composite entity, i.e., the electron plus distortion, is the polaron. When the distorted region is less than a lattice spacing (i.e., 1/2 bandwidth $<$ binding energy) we have a small polaron. The polaron propagates just like an electron. However, the hopping integral gets modified because one has to take into account the wave functions of the host molecules which correspond to displaced simple harmonic oscillators. The overlap between the simple harmonic-oscillator wave functions between adjacent sites decreases with increasing temperature because as temperature increases higher eigenfunctions with more nodes come into play. The band energy thus assumes the form $\epsilon_k\sim-2t[\cos(k_xa)+\cos(k_ya)+\cdots]\exp[-g_0^2\coth(\omega_0/2k_BT)]$ with g_0 being proportional to molecular distortion and ω_0 being the Debye energy. As can be seen the band energy at high temperatures decreases exponentially with temperature.

We are dealing with narrow band systems that are nondegenerate and hence the mobility is given by $\mu=eD/(k_BT)$ where D is the diffusivity. At higher temperatures band narrowing occurs and when coherent motion is no longer possible the electron becomes localized and propagates by hopping. The diffusivity is then given by $D\sim a^2/\tau$ where the lifetime τ, for adiabatic transport, is given by the classical result $1/\tau=\omega_0/(2\pi)\exp[-E_a/(k_BT)]$ with the activation energy $E_a=2g_0^2\tanh[\omega_0/(4k_BT)]$ (see Holstein's article[18] for details). On the other hand at low temperatures bandlike conduction is possible and the diffusivity is given by $D\propto\langle v^2\rangle\tau$ with v being the velocity and τ being still given by the above formula. The crossover from bandlike motion to hopping conductivity takes place when the uncertainty in energy $(\hbar/\tau)$ is of the order of half the bandwidth. Now, it is important to point out that the total mobility is the sum of the band and hopping mobilities (see Friedman's paper[19] for details). The total mobility is then given by

$$\mu_{Total}=\beta q_e a^2\left\{2\pi\frac{t^2}{\omega_0}\exp\left[-2g_0^2\,\mathrm{csch}\left(\frac{\beta\omega_0}{2}\right)\right]+\frac{\omega_0}{2\pi}\exp\left[-2g_0^2\tanh\left(\frac{\beta\omega_0}{4}\right)\right]\right\},\tag{1}$$

where q_e is the electronic charge and $\beta=1/(k_BT)$.

When we include Hund's coupling, t gets modified to be $t\sqrt{(1+M^2/M_S^2)/2}$. Now when a magnetic field gets switched on, the value of the effective hopping integral increases, the lattice gets less distorted (effective g_0 decreases), resistivity decreases, and bandlike motion persists longer (i.e., the peak position of the resistivity shifts to higher temperatures). Thus the system can have a large drop in resistivity at T_C when a magnetic field is applied.

III. ADIABATIC TRANSPORT OF SMALL POLARONS

To study transport we use the double-exchange modification to include effects due to on-site Hund's coupling between itinerant holes and localized electrons and take the total Hamiltonian to be

$$H=-t_{DE}\sum_{\langle ij\rangle}c_i^\dagger c_j+\sum_{\vec{q}}\omega_{\vec{q}}a_{\vec{q}}^\dagger a_{\vec{q}}+\frac{1}{N^{1/2}}\sum_{j,\vec{q}}c_j^\dagger c_j e^{i\vec{q}\cdot\vec{R}_j}g_{\vec{q}}\omega_{\vec{q}}(a_{\vec{q}}+a_{-\vec{q}}^\dagger),\tag{2}$$

where $c_j(a_{\vec{q}})$ is the hole (phonon) destruction operator, $\langle ij\rangle$ corresponds to nearest neighbors, $\omega_{\vec{q}}$ is the optical phonon frequency $(\hbar=1)$, $g_q\omega_{\vec{q}}$ is the hole-phonon coupling, and $t_{DE}=t\sqrt{(1+M^2/M_S^2)/2}$, M is the magnetization, M_S is the saturated magnetization, and N is the number of sites. Here it should be mentioned that by allowing only one electron per site the restriction on two electrons of opposite spin to occupy the same site is equivalent to Pauli blocking and can be more severe than hard core repulsion (i.e., it can lead to higher energies). Furthermore the above Hamiltonian corresponds to assuming a single orbital per site which on account of Jahn-Teller splitting may be justified. Actually, we feel that only one orbital ought to be involved in the transport process as tunneling between two similar potential wells is more likely than between two dissimilar potential wells (i.e., tunneling between same orbitals is more likely because of resonant tunneling). Then the electron lowers its energy better through enhanced hopping or lower kinetic energy. Fur-

thermore, the experiments of Lanzara *et al.*[20] are in agreement with our claims. We will elaborate on this after we present our polaronic picture.

We will first outline the procedure for obtaining the resistivity for the case where the hopping term is small compared to the binding energy (i.e., the true small polaron case) and then proceed to incorporate finite bandwidth effects. We will now perform the so-called Lang-Firsov transformation[21] $\tilde{H}=e^{S}He^{-S}$ to diagonalize the Hamiltonian with

$$S=-\sum_{j,\vec{q}} c_j^{\dagger}c_j e^{i\vec{q}\cdot\vec{R}_j}\frac{g_{\vec{q}}}{N^{1/2}}(a_{\vec{q}}-a_{-\vec{q}}^{\dagger}). \tag{3}$$

The resulting Hamiltonian is given by

$$\tilde{H}=-t_{DE}\sum_{\langle ij\rangle} c_i^{\dagger}c_j X_i^{\dagger}X_j+\sum_{\vec{q}} \omega_{\vec{q}}a_{\vec{q}}^{\dagger}a_{\vec{q}}-\sum_{j,\vec{q}}\frac{g_{\vec{q}}^2\omega_{\vec{q}}}{N}c_j^{\dagger}c_j, \tag{4}$$

where

$$X_j=\exp\left[\sum_{\vec{q}} e^{i\vec{q}\cdot\vec{R}_j}\frac{g_{\vec{q}}}{N^{1/2}}(a_{\vec{q}}-a_{-\vec{q}}^{\dagger})\right], \tag{5}$$

and $\Sigma_{\vec{q}}(g_{\vec{q}}^2\omega_{\vec{q}}/N)$ is the binding energy. Here it should be pointed out that to obtain the above transformed Hamiltonian we have used the following approximation:

$$\sum_{j,k,\vec{q}}\frac{g_{\vec{q}}^2\omega_{\vec{q}}}{N}c_j^{\dagger}c_j e^{i\vec{q}\cdot(\vec{R}_j-\vec{R}_k)}c_k^{\dagger}c_k=\sum_{j,\vec{q}}\frac{g_{\vec{q}}^2\omega_{\vec{q}}}{N}c_j^{\dagger}c_j. \tag{6}$$

The above relationship is exact when $g_{\vec{q}}^2\omega_{\vec{q}}$ is independent of $\vec{q}$.

The single small polaron eigenstate of the Hamiltonian in Eq. (2) is given by

$$|\psi_i\rangle=e^{-S}|i\rangle|\ldots n_{\vec{q}}\ldots\rangle=|i\rangle X_i|\ldots n_{\vec{q}}\ldots\rangle, \tag{7}$$

where $|i\rangle$ is the molecular orbital eigenstate at site i and $|\ldots n_{\vec{q}}\ldots\rangle$ is the product of the eigenstates of the molecules at various sites executing simple harmonic motion with phononic occupation number $n_{\vec{q}}$. The above wave function is exact in the limit of the ratio of the hopping term to the binding energy being vanishingly small.

In Eq. (4) the first term involving the hopping term is the small parameter. If the dominant transport mechanism corresponds to diagonal processes (i.e., number of phonons in each state $\vec{q}$ remains unchanged) phase coherence is maintained when the particle propagates. In fact then the particle moves like a Bloch electron and forms energy bands with energy being given by the thermal average of the first term in Eq. (4) (see Appendix A for details).

$$\begin{aligned}-\left\langle t_{DE}\sum_{\langle ij\rangle} c_i^{\dagger}c_j X_i^{\dagger}X_j\right\rangle &= -2t_{DE}\sum_{\vec{k}}[\cos(k_x a)+\cos(k_y a)+\cdots]n_{\vec{k}}\langle X_i^{\dagger}X_j\rangle\\ &= -2t_{DE}\sum_{\vec{k}}[\cos(k_x a)+\cos(k_y a)+\cdots]n_{\vec{k}}\\ &\quad\times\exp[-g_0^2\coth(\beta\omega_0/2)]\\ &= \sum_{\vec{k}}\epsilon_{\vec{k}}n_{\vec{k}},\end{aligned} \tag{8}$$

where $n_{\vec{k}}=\langle c_{\vec{k}}^{\dagger}c_{\vec{k}}\rangle$ and $\langle\ldots\rangle$ corresponds to thermal average.

We will now calculate the conductivity for localized states, i.e., the hopping conductivity. The polarization operator is given by $\vec{P}=\Sigma_i\vec{R}_i c_i^{\dagger}c_i$. Then the current operator is given by

$$\vec{j}=q_e\frac{\partial\vec{P}}{\partial t}=\frac{q_e i}{\hbar}[\tilde{H},\vec{P}]=-\frac{iq_e t_{DE}}{\hbar}\sum_{\langle ij\rangle}[\vec{R}_i-\vec{R}_j]c_i^{\dagger}c_j X_i^{\dagger}X_j. \tag{9}$$

Using the above form of the current operator and the many-body states obtained from the single-particle states $|i\rangle|\ldots n_{\vec{q}}\ldots\rangle$ and taking $\omega_{\vec{q}}=\omega_0$ and $g_{\vec{q}}=g_0$, we can obtain the conductivity to be (see Appendix B)

$$\begin{aligned}\mathrm{Re}(\sigma_{\alpha\alpha})&=\frac{1-e^{-\beta\omega}}{2\omega}\int_{-\infty}^{\infty}dt\,e^{i\omega t}\langle j_\alpha(t)j_\alpha(0)\rangle\\ &=\frac{n_c q_e^2 a^2}{k_B T}\frac{\sqrt{\pi}t_{DE}^2}{g_0\omega_0\sqrt{\mathrm{cosech}\,\omega_0\beta/2}}e^{-2g_0^2\tanh(\beta\omega_0/4)},\end{aligned} \tag{10}$$

where n_c is the density of carriers. Furthermore, it should be noted that we need $2g_0^2\,\mathrm{csch}(\beta\omega_0/2)\gg 1$ for Eq. (10) to be valid. Now the mobility, for a system of nondegenerate electrons, is given by the Einstein relation $\mu=q_e D\beta$ where D is the diffusivity. In the region of interest, i.e., around the metal-insulator transition, we expect band narrowing to be sufficiently strong so that the Fermi energy is not much larger than the thermal energy. Since the hopping-regime diffusivity is given by $D_{hop}=a^2/(6\tau)$, we readily obtain the scattering time τ to be

$$\frac{1}{6\tau}=\frac{\sqrt{\pi}t_{DE}^2}{g_0\omega_0\sqrt{\mathrm{cosech}\,\omega_0\beta/2}}e^{-2g_0^2\tanh(\beta\omega_0/4)}. \tag{11}$$

The above expression for τ corresponds to the nonadiabatic regime (or $t\ll\omega_0$). As for the adiabatic case, τ is given by

$$\frac{1}{6\tau}=\frac{\omega_0}{2\pi}e^{-2g_0^2\tanh(\beta\omega_0/4)}, \tag{12}$$

which for high temperatures reduces to the classical case

$$\frac{1}{6\tau}=\frac{\omega_0}{2\pi}e^{-g_0^2\omega_0\beta/2}, \tag{13}$$

with $g_0^2\omega_0/2$ corresponding to the activation energy.

The diffusivity for band conduction is given by

$$D_{band}=\langle|\vec{\nabla}E_{\vec{k}}|^2\tau\rangle/d=2\tau a^2 t_{DE}^2 e^{-2g_0^2\coth(\beta\omega_0/2)}, \tag{14}$$

where d is the dimension of the system and τ is given by the same expression as in the hopping case.[22]

Then based on Friedman's work[19] we take the total mobility (μ_T) to be the sum of the band mobility and the hopping mobility and hence the total resistivity ($1/\rho = n_c q_e \mu_T$) to be given by

$$\frac{4\pi}{n_c q_e^2 a^2 \rho} = \beta\omega_0 \left\{ \frac{8\pi^2}{3} \frac{t^2}{\omega_0^2} \exp\left[-2\,\theta\,\mathrm{cosech}\left(\frac{\beta\omega_0}{2}\right)\right] + \left(1 + \frac{M^2}{M_S^2}\right) \exp\left[-2\,\theta \tanh\left(\frac{\beta\omega_0}{4}\right)\right]\right\}, \quad (15)$$

where $\theta = g_0^2$. Here we note that Friedman's analysis also accounts for how an electron may seem localized yet it can have translation invariance symmetry intact—the reason being that the mobility is the sum of the hopping and bandlike mobilities and hence will always have a component, no matter how small, that is metallic.

IV. SMALL POLARON PICTURE WITH FINITE BANDWIDTH EFFECTS

We will now include finite bandwidth effects in our small polaronic picture. However, we will still treat the ratio $t_{DE}/2g_0^2\omega_0$ as small. The polaronic wave function now spreads and barely extends to the nearest-neighboring sites. Then the eigenstate of the nearly small polaron is given by (see Toyozawa's paper also[14])

$$|\Psi_i\rangle = \sum_j B(j)|i-j\rangle \tilde{X}_i |\ldots n_{\vec{q}} \ldots\rangle, \quad (16)$$

where $\tilde{X}_i$ is given by

$$\tilde{X}_i = \exp\left[\sum_{\vec{q}} e^{i\vec{q}\cdot\vec{R}_i} \alpha_{\vec{q}} (a_{\vec{q}} - a^\dagger_{-\vec{q}})\right]. \quad (17)$$

In the above equation $B(j) = 0$ for $|\vec{R}_j| > a$. Furthermore $B(j)$ and $\alpha_{\vec{q}}$ are to be determined by minimizing the single small polaronic energy. Upon taking the expectation value of the Hamiltonian with respect to a small polaron state of momentum $\vec{k}$ given by $|\Psi_{\vec{k}}\rangle = \Sigma_i e^{\vec{k}\cdot\vec{R}_i}|\Psi_i\rangle$ one gets

$$-\langle\Psi_{\vec{k}}| t_{DE} \sum_{\langle ij\rangle} c_i^\dagger c_j |\Psi_{\vec{k}}\rangle \approx -t_{DE} \sum_{\delta,i} B(i)B(i-\delta) \quad (18)$$

and

$$\langle\Psi_{\vec{k}}| \sum_{\vec{q}} \omega_{\vec{q}} a_{\vec{q}}^\dagger a_{\vec{q}} + \frac{1}{N^{1/2}} \sum_{j,q} c_j^\dagger c_j e^{i\vec{q}\cdot\vec{R}_j} g_{\vec{q}} \omega_{\vec{q}} (a_{\vec{q}} + a^\dagger_{-\vec{q}}) |\Psi_{\vec{k}}\rangle$$

$$\approx \sum_{\vec{q}} \omega_{\vec{q}} (N_{\vec{q}} + \alpha_{\vec{q}}^2) - 2N^{-1/2} \sum_{\vec{q},i} \alpha_{\vec{q}} \omega_{\vec{q}} g_{\vec{q}} \times \cos(\vec{q}\cdot\vec{R}_i) B^2(i), \quad (19)$$

where we have neglected the small valued vibrational overlap factors $\langle \ldots n'_{\vec{q}} \ldots |\tilde{X}_i^\dagger \tilde{X}_j| \ldots n_{\vec{q}} \ldots\rangle$ for $i \neq j$. Upon minimizing the polaron energy with respect to $\alpha_{\vec{q}}$ one obtains

$$\alpha_{\vec{q}} = N^{-1/2} g_{\vec{q}} \left[\sum_j B(j)^2 \cos(\vec{q}\cdot\vec{R}_j)\right]. \quad (20)$$

For small values of $t_{DE}/2g_0^2\omega_0$, on using the constraint that $\Sigma_j B^2(j) = 1$, one obtains from the above equations $B(0) \approx 1$ and

$$B(j) \approx \frac{t_{DE}}{2N^{-1} \sum_{\vec{q}} \omega_{\vec{q}} g_{\vec{q}}^2 [1 - \cos(\vec{q}\cdot\vec{R}_j)]}, \quad (21)$$

for $|\vec{R}_j| = a$. The above results are similar to those obtained by Gosar.[23]

Using the above eigenstate $|\Psi_i\rangle$ for the small polaronic state and again using the procedure outlined in Appendix B for deriving the conductivity in the localized regime, one obtains [on neglecting $B(j)$ for $j \neq 0$ due to its small contribution] the same expression for conductivity but with the lattice distortion g_0^2 renormalized

$$\mathrm{Re}[\sigma_{\alpha\alpha}(\omega)] = \frac{1 - e^{-\beta\omega}}{6\omega} \frac{q_e^2 t_{DE}^2}{\hbar^2} c(1-c) a^2 \frac{zN}{V} \sqrt{\pi/\tilde{\gamma}} \times e^{-2\tilde{S}_T + \tilde{\phi}(-i\beta/2) + \omega\beta/2 - \omega^2/(4\tilde{\gamma})}, \quad (22)$$

where

$$\tilde{S}_T \equiv \sum_{\vec{q}} \frac{|\tilde{\lambda}_{\vec{q}}|^2}{2} \coth\frac{\beta\omega_{\vec{q}}}{2}, \quad (23)$$

$$\tilde{\phi}(t) = \sum_{\vec{q}} |\tilde{\lambda}_{\vec{q}}|^2 [(N_{\vec{q}} + 1) e^{-i\omega_{\vec{q}} t} + N_{\vec{q}} e^{i\omega_{\vec{q}} t}], \quad (24)$$

and

$$\tilde{\gamma} = \sum_{\vec{q}} |\tilde{\lambda}_{\vec{q}}|^2 [N_{\vec{q}}(N_{\vec{q}} + 1)]^{1/2} \omega_{\vec{q}}^2, \quad (25)$$

with $\tilde{\lambda}_{\vec{q}} = e^{i\vec{q}\cdot\vec{R}_j}(1 - e^{i\vec{q}\cdot\vec{\delta}})\alpha_{\vec{q}}$. Here it should be pointed out that the authors of Ref. 10 did not take into account the renormalization of $\lambda_{\vec{q}}$ due to the finite bandwidth effects. They also failed to recognize that $\tilde{\gamma}\beta \gg |\epsilon_{\vec{k}} - \epsilon_{\vec{p}}|$, while evaluating the integral with respect to time in order to obtain the expression for conductivity.

Now, upon taking $\omega_{\vec{q}} = \omega_0$ and $g_{\vec{q}} = g_0$, one obtains the same expression for the total resistivity given by Eq. (15) where θ is expressed as follows:

$$\theta \equiv g_0^2 \left[1 - \frac{(z+1)t_{DE}^2}{2g_0^4\omega_0^2}\right], \quad (26)$$

with z being the coordination number.[24] Here, it should be noted that we need $2\,\theta\,\mathrm{csch}(\beta\omega_0/2) \gg 1$ for Eq. (15) to be valid. Furthermore, the optical conductivity above the metal-insulator transition (where only the conductivity due to localized carriers dominates) is given by

$$\frac{\mathrm{Re}[\sigma_{\alpha\alpha}(\omega)]}{\sigma_{\alpha\alpha}(\omega \to 0)} = \frac{\sinh(\beta\omega/2)}{\beta\omega/2} e^{-\omega^2/(4\widetilde{\gamma_0})}, \quad (27)$$

where $\widetilde{\gamma_0} = \theta\omega_0^2\,\mathrm{cosech}(\beta\omega_0/2)$. We note, from Eq. (27), that the optical conductivity scaled by the dc conductivity depends only on the parameter $\widetilde{\gamma_0}$.

We will now study the magnetic transition within a mean-field approximation. The magnetization ratio M/M_S is not

very sensitive to the type of approximation (see Ref. 25 for a weak Hund's coupling treatment of the magnetization problem). The magnetization ratio is given by

$$S\frac{M}{M_S} = -\frac{\sum_{S_z} S_z \exp[-g\mu_B H_{eff} S_z \beta]}{\sum_{S_z} \exp[-g\mu_B H_{eff} S_z \beta]}, \tag{28}$$

with $H_{eff} = \lambda(M/M_S)$. On using the condition that as $T \to T_C$ we have $M/M_S \to 0$, we get for $S = 3/2$ the relation $\lambda g \mu_B = 1.2 k_B T_C$. Estimating the transition temperature T_C with accuracy is difficult and we will only give an order of magnitude estimate for it and will provide a qualitative feel for its dependence on various physical parameters of the system. Above the transition point the electrons are localized and form small ferromagnetic domains (or magnetic polarons) so as to minimize the free energy. At the transition point the magnetic polarons align to give a ferromagnetic phase whose size is of the order of the size of the system. At this point the decrease in kinetic energy because of the electronic delocalization is equal to the increase in the entropic contribution to the free energy as given below.[26]

$$-N\delta 6 t_{DE} e^{-\theta \coth(\beta\omega_0/2)} \approx -N k_B T_C \ln 4. \tag{29}$$

V. RESULTS AND DISCUSSION

In the doping regime where the manganites are insulating (i.e., $\delta \sim 0$ or $\delta > 0.5$), although there is orbital order and both orbitals enter the Hamiltonian, in the doping regime $0.2 < \delta < 0.4$ where CMR is observed only one orbital need be considered. As described in a recent interesting paper by Khomskii,[27] the manganite system tries to lower its overall energy by entering into a ferromagnetic orbitally ordered state with the same orbital being occupied at each site. The situation is similar to what is encountered in Nagaoka-type ferromagnetism in spin systems. When doped with a few holes, just as an antiferromagnetic spin state can become ferromagnetic so will an orbitally aniferromagnetic state become an orbitally ferromagnetic one. In Ref. 27, it is also pointed out that at sizeable doping a state with $d_{x^2-y^2}$ or d_{z^2} ordering may have lower energy than the proposed state where only $d_{z^2} \pm i d_{x^2-y^2}$ orbitals are occupied.

Based on the experimental results of Lanzara *et al.*[20] we will now try to justify that only one of the orbitals d_{z^2} or $d_{x^2-y^2}$ is occupied and that the orbital ordering temperature is higher than the magnetic transition temperature T_C (which is possible because there is no reason to expect coupling between the order parameters for the magnetic transition and the orbital ordering transition). In Ref. 20, in Fig. 4 we see that only one type of distortion of the octahedron (the so-called Q_3 normal mode) seems to be relevant both above and below T_C. However, there are two distortions of this same type (at sites A and B) above T_C but their degree of distortion is different. We think that it indicates that the lattice distortion is less in the ferromagnetic domains (site A) that exist even above T_C and is similar to the distortion (again of the same Q_3 type) in the ferromagnetic region below T_C at $T < 200$ K. Moreover, in the paramagnetic regime (site B) the distortion is expected to be more in our picture because the effective hopping integral t_{DE} is smaller in this regime. Furthermore, from Fig. 2 of Ref. 20 we see that even at $T = 300$ K ($> T_C = 240$ K) only Q_3 mode exists which prompts us to conclude that the orbital ordering probably occurs at a fairly higher temperature than T_C. It is also of interest to note from Fig. 3 of Ref. 20 that extended x-ray absorption fine-structure probes instantaneous and local distortions that are larger than the ones observed from diffraction experiments. This may explain why other probes (like neutron scattering) do not show noticeable Jahn-Teller distortion at low temperatures.

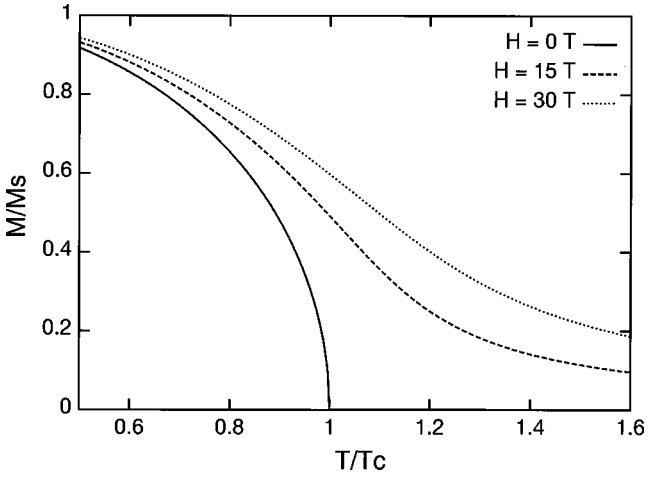

FIG. 1. Plot of the magnetization ratio M/M_S versus the reduced temperature T/T_C at magnetic fields $H = 0$ T, $H = 15$ T, and $H = 30$ T.

Our magnetization curves M/M_S as a function of the reduced temperature T/T_C (see Fig. 1) are independent of the values of the various parameters of the system like t, δ, ω_0, and g_0 because of the mean-field nature of the approximation. The qualitative behavior of the experimental curves is mimicked by our calculations but the experimental values of M/M_S rise faster with T/T_C (see Ref. 15).

The peak in the resistivity occurs when the system goes from insulating behavior to a metallic behavior (however, the peak need not occur exactly when the hopping mobility becomes equal to the band mobility). When the system becomes metallic the system also becomes ferromagnetic because the itinerant electrons polarize the localized spins. Thus we can take the metal-insulator transition point as also the magnetic transition point—a fact borne out by experiments (see Ref. 15).

From the expression for the resistivity [see Eq. (15)] it follows that for a given value of t/ω_0, the ratio $k_B T_C/\omega_0$ is fixed and one need not treat ω_0 as a variable when studying resistance dependence on various parameters.

We will now discuss the resistivity given by Eq. (15). The conduction goes from a hopping type at high temperatures to a band type at low temperatures. In Fig. 2 we have shown the dependence of resistivity ρ on temperature at various magnetic fields. The values of the hopping integral t are taken such that the bandwidth lies in the range 1 eV$-$3.5 eV which is a realistic range based on band-structure calculations. The values of g_0^2 are taken from the experimentally obtainable activation energy ($\theta\omega_0/2$) values corresponding to temperatures in the range 1000 K$-$2500 K (see Refs. 1,12), while

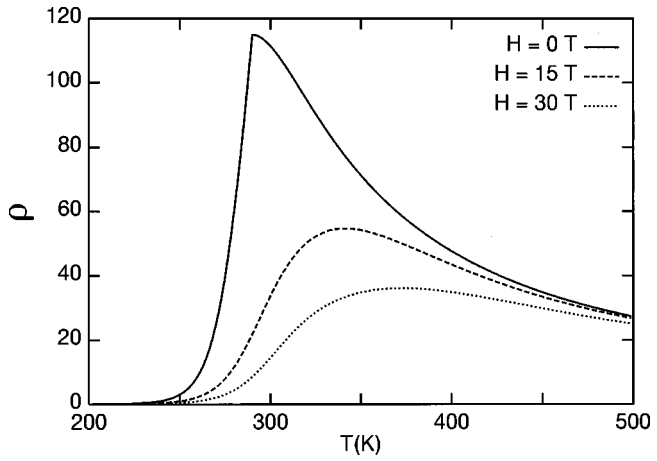

FIG. 2. Plot of the resistivity ρ in units of $4\pi/(n_c q_e^2 a^2)$ versus temperature T in three dimensions for adiabaticity parameter $t/\omega_0=6$, $g_0^2=12$, Debye temperature $T_D=500$ K, and for the following magnetic fields: (i) $H=0$ T; (ii) $H=15$ T; and (iii) $H=30$ T.

the chosen value of the Debye temperature $T_D=500$ K is realistic, too (see Ref. 1). The general trend of the resistivity including the drop at the MI transition at $H=0$ T is similar to the experimental results.[15] On introducing a magnetic field the system gets magnetized at temperatures higher than T_C and thus the value of θ is smaller [see Eq. (26)]. Consequently, the resistivity is smaller and $T_{\rho^{max}}$ (the temperature at which resistivity becomes maximum) increases.

For $T \geqslant T_C$, when $D_{band}/D_{hop} \gg 1$ the magnetoresistance $\Delta\rho(H) \equiv [\rho(0)-\rho(H)]/\rho(0)$ is given by [see Eqs. (15) and (26)]

$$\Delta\rho(H) \approx 1 - \exp\left[-\frac{(z+1)}{2g_0^2}\frac{t^2}{\omega_0^2}\frac{M^2}{M_S^2}\operatorname{csch}\left(\frac{\beta\omega_0}{2}\right)\right], \quad (30)$$

and when $D_{band}/D_{hop} \ll 1$ it is given by

$$\Delta\rho(H) \approx 1 - \frac{\exp\left[-\frac{(z+1)}{2g_0^2}\frac{t^2}{\omega_0^2}\frac{M^2}{M_S^2}\tanh\left(\frac{\beta\omega_0}{4}\right)\right]}{1+(M/M_S)^2}. \quad (31)$$

For $\beta\omega_0/2<1$, on taking $\operatorname{csch}(\beta\omega_0/2) \approx 2/(\beta\omega_0)$ and $\tanh(\beta\omega_0/4) \approx \beta\omega_0/4$, if $\theta\beta\omega_0/2>1$ the following can be shown: (i) $T_{\rho_M^{max}}$ increases as g_0^2 decreases (or t^2/ω_0^2 increases); and (ii) for fixed values of g_0^2 and t^2/ω_0^2 and for large enough

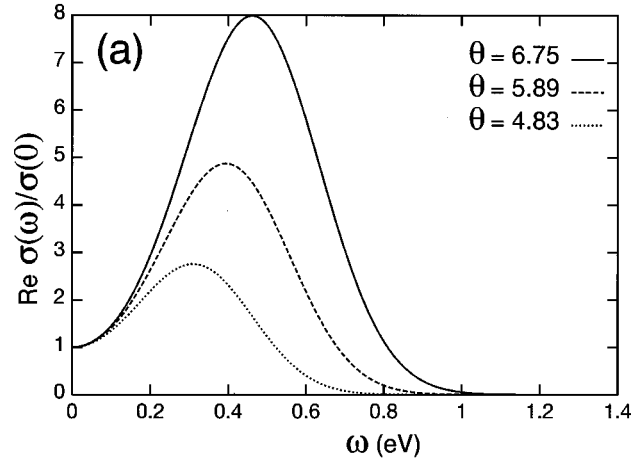

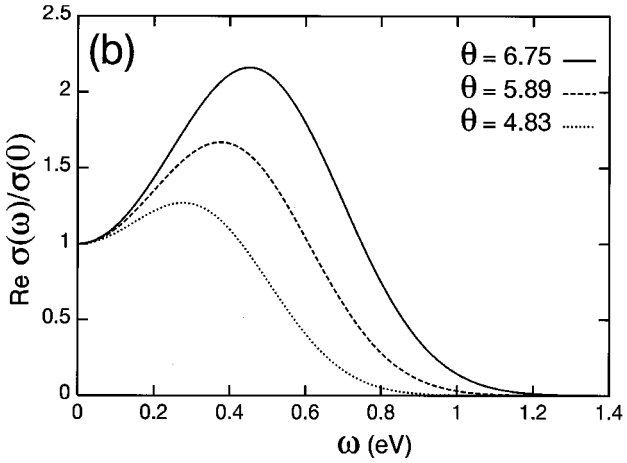

FIG. 3. Plot of the scaled optical conductivity $\mathrm{Re}\sigma(\omega)/\sigma(0)$ as a function of frequency at various values of the renormalized electron-phonon coupling parameter θ and for: (a) $T=300$ K ($\approx T_C$) and (b) $T=500$ K. In Table I, $\theta=6.75$ corresponds to $t/\omega_0=6$ and $g_0^2=12$; $\theta=5.89$ corresponds to $t/\omega_0=4$ and $g_0^2=9$; and $\theta=4.83$ corresponds to $t/\omega_0=2$ and $g_0^2=6$.

$$\frac{(z+1)}{2g_0^2}\frac{t^2}{\omega_0^2},$$

$T_{\rho^{max}}$ increases as M increases. The above observations are borne out by the numerical results reported in Table I where the empty boxes correspond to cases where our approximation may not be good. We further note that for the same value of the polaron size parameter $t/(\omega_0 g_0^2)$ the magnetoresistance $\Delta\rho(H)$ increases as the adiabaticity parameter t/ω_0 increases.

In Fig. 3, we plot the scaled optical conductivity

TABLE I. Calculated values of the transition temperature T_C and magnetoresistance $\Delta\rho(H)$ at T_C for $T_D=500$ K, various values of t/ω_0 and g_0^2, and magnetic fields $H=15$ T and $H=30$ T.

	$g_0^2=6$			$g_0^2=9$			$g_0^2=12$		
t/ω_0	$\Delta\rho(15\text{ T})$	$\Delta\rho(30\text{ T})$	T_C	$\Delta\rho(15\text{ T})$	$\Delta\rho(30\text{ T})$	T_C	$\Delta\rho(15\text{ T})$	$\Delta\rho(30\text{ T})$	T_C
2	37%	49%	297 K	34%	45%	245 K	31%	41%	228 K
3	46%	62%	400 K	48%	62%	264 K	44%	57%	237 K
4				62%	77%	295 K	58%	72%	248 K
6							81%	93%	290 K

$\mathrm{Re}\sigma(\omega)/\sigma(0)$ [given by Eq. (27)] as a function of the frequency at different temperatures. The maximum of the optical conductivity occurs at $\omega \approx \tilde{\gamma}_0 \beta$ as expected from the formula in Eq. (27). We note that as the value of the renormalized electron-phonon coupling parameter θ increases, the optical conductivity curve spreads out more. We also find that, as the temperature increases the value of the scaled optical conductivity decreases. Furthermore, the calculated scaled curves are in qualitative agreement with experiments. In the experimental situation there are two pieces to the conductivity—one coming from transitions with electrons parallel to the core spins ($\omega \sim t$) and another at higher energy ($\omega \sim$ twice the Hund's coupling energy) involving transitions to states where the electron spins are antiparallel to the core spins. However, since we do not allow for double occupancy at any site, the second piece of the optical conductivity does not appear in our calculated curves.

In conclusion, we say that we showed the importance of finite bandwidth effects in understanding CMR within a small polaron picture. In addition to the polaron size parameter studied by other authors,[8] we have also identified another dimensionless parameter (the adiabaticity parameter) and demonstrated its importance. The values of magnetoresistance calculated by us compare favorably with the experimentally reported ones.

ACKNOWLEDGMENTS

The author would like to thank C. S. Ting, T. V. Ramakrishnan, H. R. Krishnamurthy, V. Pai, D. D. Sarma, Ram Seshadri, Jinwu Ye, G. F. Giuliani, and A. N. Das for discussions. The author would also like to acknowledge useful discussions with D. Khomskii regarding the validity of considering only one orbital in the doping regime where CMR occurs. This work was partially supported by Texas Center for Superconductivity and a grant from Texas ARP (ARP-003652-0241-1999).

APPENDIX A

In this appendix we will derive the band narrowing due to phonons. The number of phonons in each state $\vec{q}$ remains unchanged in a diagonal transition. If this is the dominant mechanism, then phase coherence is maintained and the electron propagates as a bandlike particle. Using the decoupling scheme $\langle c_i^\dagger c_j X_i^\dagger X_j \rangle = \langle c_i^\dagger c_j \rangle \langle X_i^\dagger X_j \rangle$ one obtains the single-particle energy to be

$$\begin{aligned}\epsilon_{\vec{k}} &= -2t_{DE}[\cos(k_x a)+\cos(k_y a)+\cdots]\langle X_{j+\delta}^\dagger X_j\rangle \\ &= -2t_{DE}(\cos(k_x a)+\cos(k_y a)+\cdots) \\ &\quad \times \exp[-g_0^2 \coth(\beta\omega_0/2)],\end{aligned} \tag{A1}$$

where $|\vec{R}_\delta| = a$. We will now proceed to derive the above expression. Now

$$\langle X_{j+\delta}^\dagger X_j \rangle = \Pi_{\vec{q}} \langle e^{\lambda_{\vec{q}} a_{\vec{q}} - \lambda_{\vec{q}}^\star a_{\vec{q}}^\dagger} \rangle, \tag{A2}$$

where $\lambda_{\vec{q}} = e^{i\vec{q}\cdot\vec{R}_j}(1-e^{i\vec{q}\cdot\vec{\delta}})g_{\vec{q}}/N^{1/2}$. Then the thermal average is given by

$$\langle X_{j+\delta}^\dagger X_j \rangle = \Pi_{\vec{q}} \frac{\sum_{n_{\vec{q}}=0}^{\infty} \langle n_{\vec{q}}| e^{-\beta n_{\vec{q}}\omega_{\vec{q}}} e^{-|\lambda_{\vec{q}}|^2/2} e^{-\lambda_{\vec{q}}^\star a_{\vec{q}}^\dagger} e^{\lambda_{\vec{q}} a_{\vec{q}}} |n_{\vec{q}}\rangle}{\sum_{n_{\vec{q}}=0}^{\infty} \langle n_{\vec{q}}| e^{-\beta n_{\vec{q}}\omega_{\vec{q}}} |n_{\vec{q}}\rangle}. \tag{A3}$$

On noting that

$$e^{ua}|n\rangle = \sum_{l=0}^{\infty} \frac{u^l}{l!} a^l |n\rangle, \tag{A4}$$

with

$$a^l|n\rangle = \left[\frac{n!}{(n-l)!}\right]^{1/2} |n-l\rangle, \tag{A5}$$

we get the following relationship:

$$\langle n| e^{-u^\star a^\dagger} e^{ua} |n\rangle = \sum_{l=0}^{n} \frac{(-|u|^2)^l}{(l!)^2}\left[\frac{n!}{(n-l)!}\right] = L_n(|u|^2), \tag{A6}$$

where $L_n(x)$ is the Laguerre polynomial. Since the following identity holds:

$$\sum_{l=0}^{\infty} L_n(|u|^2) z^l = \frac{e^{[|u|^2 (z/z-1)]}}{1-z}, \tag{A7}$$

we obtain from Eqs. (A3)–(A7)

$$\begin{aligned}\langle X_{j+\delta}^\dagger X_j \rangle &= \Pi_{\vec{q}} e^{-|\lambda_{\vec{q}}|^2/2} e^{-|\lambda_{\vec{q}}|^2 N_{\vec{q}}} \\ &= \exp\left[-\sum_{\vec{q}} (|\lambda_{\vec{q}}|^2/2) \coth\left(\frac{\beta\omega_{\vec{q}}}{2}\right)\right] \\ &\equiv e^{-S_T},\end{aligned} \tag{A8}$$

with $N_{\vec{q}}$ being the Bose-Einstein distribution function. Then for $\omega_{\vec{q}} = \omega_0$ and $g_{\vec{q}} = g_0$ we obtain Eq. (A1).

APPENDIX B

In this appendix we will calculate the conductivity within the small polaron picture in the hopping regime.

$$\mathrm{Re}[\sigma_{\alpha\alpha}(\omega)] = \frac{1-e^{-\beta\omega}}{2\omega}\int_{-\infty}^{\infty} dt e^{i\omega t}\langle j_\alpha(t) j_\alpha(0)\rangle$$

$$= \frac{e^2 t_{DE}^2}{\hbar^2}\frac{1-e^{-\beta\omega}}{6\omega}\sum_{\vec{\delta},\vec{\delta}',j,j'}\vec{\delta}\cdot\vec{\delta}'\int_{-\infty}^{\infty} dt e^{i\omega t}\langle c_j^\dagger(t) c_{j+\delta}(t) c_{j'+\delta'}^\dagger c_{j'}\rangle\langle X_j^\dagger(t) X_{j+\delta}(t) X_{j'+\delta'}^\dagger X_{j'}\rangle. \tag{B1}$$

In the above equation, the dominant contribution is obtained when $j=j'$ and $\delta=\delta'$. The first correlation function in the above equation can be approximated by

$$\langle c_j^\dagger(t) c_{j+\delta}(t) c_{j+\delta}^\dagger c_j\rangle = \frac{1}{N^2}\sum_{\vec{k},\vec{p}} f_{\vec{k}}(1-f_{\vec{p}}) e^{i(\epsilon_{\vec{k}}-\epsilon_{\vec{p}})t}, \tag{B2}$$

where $f_{\vec{p}}$ is the Fermi-Dirac distribution function. Now

$$\langle X_j^\dagger(t) X_{j+\delta}(t) X_{j+\delta}^\dagger X_j\rangle = \frac{\mathrm{Tr}\{e^{-\beta\tilde{H}} e^{i\tilde{H}t} X_j^\dagger X_{j+\delta} e^{-i\tilde{H}t} X_{j+\delta}^\dagger X_j\}}{\mathrm{Tr}\{e^{-\beta\tilde{H}}\}}$$

$$= \Pi_{\vec{q}} \frac{\sum_{n_{\vec{q}}=0}^{\infty}\langle n_{\vec{q}}| e^{-\beta n_{\vec{q}}\omega_{\vec{q}}} e^{-|\lambda_{\vec{q}}|^2/2} e^{\lambda_{\vec{q}}^\star a_{\vec{q}}^\dagger e^{i\omega_{\vec{q}}t}} e^{-\lambda_{\vec{q}} a_{\vec{q}} e^{-i\omega_{\vec{q}}t}} e^{-|\lambda_{\vec{q}}|^2/2} e^{-\lambda_{\vec{q}}^\star a_{\vec{q}}^\dagger} e^{\lambda_{\vec{q}} a_{\vec{q}}}|n_{\vec{q}}\rangle}{\sum_{n_{\vec{q}}=0}^{\infty}\langle n_{\vec{q}}| e^{-\beta n_{\vec{q}}\omega_{\vec{q}}}|n_{\vec{q}}\rangle}$$

$$= \Pi_{\vec{q}}(1-e^{-\beta\omega_{\vec{q}}}) e^{-|\lambda_{\vec{q}}|^2(1-e^{-i\omega_{\vec{q}}t})} \sum_{n_{\vec{q}}=0}^{\infty} e^{-\beta n_{\vec{q}}\omega_{\vec{q}}}\langle n_{\vec{q}}| e^{\lambda_{\vec{q}}^\star a_{\vec{q}}^\dagger (e^{i\omega_{\vec{q}}t}-1)} e^{-\lambda_{\vec{q}} a_{\vec{q}}(e^{-i\omega_{\vec{q}}t}-1)}|n_{\vec{q}}\rangle$$

$$= \Pi_{\vec{q}} e^{-|\lambda_{\vec{q}}|^2[(N_{\vec{q}}+1)(1-e^{-i\omega_{\vec{q}}t})+N_{\vec{q}}(1-e^{i\omega_{\vec{q}}t})]}, \tag{B3}$$

where, to obtain the last line, use has been made of the fact that

$$(1-e^{-\beta\omega_{\vec{q}}})\sum_{n_{\vec{q}}=0}^{\infty} e^{-\beta n_{\vec{q}}\omega_{\vec{q}}}\langle n_{\vec{q}}| e^{u^\star a^\dagger} e^{-ua}|n_{\vec{q}}\rangle = e^{-|u|^2 N_{\vec{q}}}. \tag{B4}$$

Defining

$$\phi(t) = \sum_{\vec{q}} |\lambda_{\vec{q}}|^2[(N_{\vec{q}}+1)e^{-i\omega_{\vec{q}}t} + N_{\vec{q}} e^{i\omega_{\vec{q}}t}], \tag{B5}$$

we have $\phi(t) = \Sigma_{\vec{q}} 2|\lambda_{\vec{q}}|^2[N_{\vec{q}}(N_{\vec{q}}+1)]^{1/2}\cos[\omega_{\vec{q}}(t+i\beta/2)]$ and obtain from Eq. (B3)

$$\int_{-\infty}^{\infty} dt e^{i\omega t}\langle c_j^\dagger(t) c_{j+\delta}(t) c_{j+\delta}^\dagger c_j\rangle\langle X_j^\dagger(t) X_{j+\delta}(t) X_{j+\delta}^\dagger X_j\rangle = \int_{-\infty}^{\infty} dt e^{i\omega t} e^{-2S_T} e^{\phi(t)}\langle c_j^\dagger(t) c_{j+\delta}(t) c_{j+\delta}^\dagger c_j\rangle$$

$$= \frac{1}{N^2} e^{-2S_T} e^{\phi(-i\beta/2)}\int_{-\infty}^{\infty} dt e^{i\omega t} e^{-\gamma(t+i\beta/2)^2}\sum_{\vec{k},\vec{p}} f_{\vec{k}}(1-f_{\vec{p}}) e^{i(\epsilon_{\vec{k}}-\epsilon_{\vec{p}})t}$$

$$\approx \sqrt{\pi/\gamma}\, c(1-c) e^{-2S_T+\phi(-i\beta/2)+\omega\beta/2-\omega^2/(4\gamma)}, \tag{B6}$$

where $\gamma = \Sigma_{\vec{q}}|\lambda_{\vec{q}}|^2[N_{\vec{q}}(N_{\vec{q}}+1)]^{1/2}\omega_{\vec{q}}^2$ and c is the number of carriers per unit site. In evaluating the above integral we assumed that $\Sigma_{\vec{q}}|\lambda_{\vec{q}}|^2[N_{\vec{q}}(N_{\vec{q}}+1)]^{1/2} \gg 1$ and used the saddle-point approximation. Furthermore, use has been made of the fact that $\gamma\beta \gg |\epsilon_{\vec{k}}-\epsilon_{\vec{p}}|$.[28]

[1] A.P. Ramirez, J. Phys.: Condens. Matter **9**, 8171 (1997).
[2] A.R. Bishop and H. Röder, Curr. Opin. Solid State Mater. Sci. **2**, 244 (1997).
[3] D.I. Khomskii and G.A. Sawatsky, Solid State Commun. **102**, 87 (1997).
[4] P.B. Allen and V. Perebeinos, Phys. Rev. B **60**, 10 747 (1999).
[5] P.-G. de Gennes, Phys. Rev. B **118**, 141 (1960).
[6] N. Furukawa, J. Phys. Soc. Jpn. **63**, 3214 (1994); **64**, 2734 (1995).
[7] A.J. Millis, P.B. Littlewood, and B.I. Shraiman, Phys. Rev. Lett. **74**, 5144 (1995).
[8] A.J. Millis, B.I. Shraiman, and R. Mueller, Phys. Rev. Lett. **77**, 175 (1996).
[9] H. Röder, Jun Zang, and A.R. Bishop, Phys. Rev. Lett. **76**, 1356 (1996).
[10] J.D. Lee and B.I. Min, Phys. Rev. B **55**, 12 454 (1997).
[11] M. Jaime, M.B. Salamon, M. Rubinstein, R.E. Treece, J.S. Horowitz, and D.B. Chrisey, Phys. Rev. B **54**, 11 914 (1996).
[12] D.C. Worledge, L. Miéville, and T.H. Geballe, Phys. Rev. B **57**, 15 267 (1998).
[13] We do not study localization due to nonmagnetic randomness. For a treatment of localization due to both spin disorder and nonmagnetic randomness see L. Sheng, D.Y. Xing, D.N. Sheng, and C.S. Ting, Phys. Rev. Lett. **79**, 1710 (1997); Phys. Rev. B **56**, R7053 (1997).
[14] Y. Toyozawa, Prog. Theor. Phys. **26**, 29 (1961).
[15] A. Urushibara, Y. Moritomo, T. Arima, A. Asamitsu, G. Kido, and Y. Tokura, Phys. Rev. B **51**, 14 103 (1995).
[16] M. Quijada, J. Cerne, J.R. Simpson, H.D. Drew, K.H. Ahn, A.J. Millis, R. Shreekala, R. Ramesh, M. Rajeswari, and T. Venkatesan, Phys. Rev. B **58**, 16 093 (1998).
[17] E. Muller-Hartman and E. Dagotto, Phys. Rev. B **54**, R6819 (1996).
[18] T. Holstein, Ann. Phys. (N.Y.) **8**, 343 (1959).
[19] L. Friedman, Phys. Rev. A **135**, 233 (1964).
[20] A. Lanzara, N.L. Saini, M. Brunelli, F. Natali, A. Bianconi, P.G. Radaelli, and S.-W. Cheong, Phys. Rev. Lett. **81**, 878 (1998).
[21] I.G. Lang and Yu.A. Firsov, Zh. Eksp. Teor. Fiz. **43**, 1843 (1962) [Sov. Phys. JETP **16**, 1301 (1962)].
[22] Can be justified on the grounds that τ is independent of position.
[23] P. Gosar, J. Phys. C **8**, 3584 (1975).
[24] We get the polaronic band energy by replacing g_0^2 with θ in Eq. (8).
[25] S. Yarlagadda, cond-mat/9809130 (unpublished).
[26] It should be noted that within the magnetic polarons $M \approx M_S$.
[27] D. Khomskii, cond-mat/0004034 (unpublished).
[28] In Ref. 10, the authors did not realize this fact.